Electron-nuclear double-resonance investigations on Cr^{3+} ions in natural $MgAl_2O_4$ spinel

1992 J. Phys.: Condens. Matter 4 7295

(http://iopscience.iop.org/0953-8984/4/35/012)

J. Phys.: Condens. Matter 4 (1992) 7295–7306. Printed in the UK

Electron–nuclear double-resonance investigations on Cr^{3+} ions in natural $MgAl_2O_4$ spinel

D Bravo† and R Böttcher‡

† Departamento de Física Aplicada C-IV, Universidad Autónoma de Madrid, Cantoblanco E-28049 Madrid, Spain

‡ Fachbereich Physik, Universität Leipzig, O-7010 Leipzig, Federal Republic of Germany

Received 1 April 1992

Abstract. The ENDOR spectra of Cr^{3+} ions in natural $MgAl_2O_4$ spinel have been measured at 4.2 K and the hyperfine and quadrupole interactions with the nearest-neighbour ^{27}Al nuclei and with the ^{53}Cr isotope have been investigated. The results show that Cr^{3+} has the point symmetry $\bar{3}m$, being subjected to the original trigonal expansion at the B sites, but inducing some distortion effects on its surroundings. Further, the isotropic hyperfine constant of the ^{27}Al nuclei has been analysed in an independent bonding model, showing that there is appreciable transfer of unpaired spin to the aluminium ion due to covalency.

1. Introduction

The spinel structure is usually assigned to the cubic space group $Fd3m$. The A sites (point symmetry, $\bar{4}3m$ (T_d)) are surrounded by four oxygen ions, and the B sites ($\bar{3}m$ (D_{3d})) by six oxygen ions which form a trigonally expanded octahedron along a [111] crystal direction (figure 1). In an ideal normal $MgAl_2O_4$ spinel, the Mg^{2+} ions occupy the tetrahedral A sites, and the Al^{3+} ions the octahedral B sites. In the case of real crystals it has been shown that the $MgAl_2O_4$ spinel is partially inverse (see [2] and references therein), although samples from a natural origin normally have a small inversion parameter (about 0.04).

On the other hand, during the last 20 years a great controversy on the assignation of the correct space group has arisen. The other space group proposed is $F\bar{4}3m$, with the B sites having the point symmetry $3m$ (C_{3v}) (without an inversion centre). Up to now many different techniques have been used to clarify this problem, but the results favour the space group $F\bar{4}3m$ [3–12] as much as $Fd3m$ [13–17]. In particular, in the case of the Cr^{3+} ion in $MgAl_2O_4$ spinel, which enters the B sites (figure 1), several workers [18–20] have suggested that the chromium ions would be shifted away along their local trigonal $\langle 111 \rangle$ axis, i.e. the point group of chromium would be $3m$ instead of $\bar{3}m$.

In this controversial situation we have carried out electron–nuclear double-resonance (ENDOR) experiments on Cr^{3+} ions incorporated in single crystals of natural $MgAl_2O_4$ spinel, in order to investigate the magnetic interaction of the unpaired spins of the Cr^{3+} ion with the surrounding nuclear spins of the 100%-abundant ^{27}Al nuclei ($I = \frac{5}{2}$), as well as with the 9.50%-abundant ^{53}Cr isotope ($I = \frac{3}{2}$). This study

0953-8984/92/357295+12$04.50

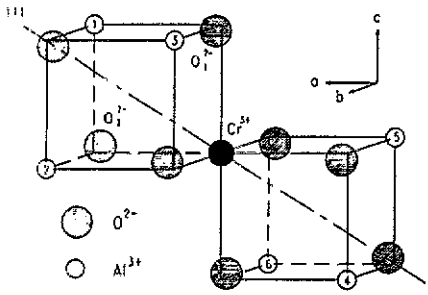

Figure 1. Partial scheme of the $MgAl_2O_4$ lattice, with the space group $Fd3m$, showing the surroundings of the B sites (where chromium enters) and the system (a, b, c) of cubic axes. In pure $MgAl_2O_4$ the oxygen atoms are shifted from the corners of the cube towards its centre, forming a trigonally expanded octahedron along the $\langle 111 \rangle$ direction. The distances are 1.928 Å from oxygen to aluminium and 2.857 Å from aluminium to aluminium. (After [1].)

allows direct determination of the local symmetry of chromium and provides reliable estimates of spin transfer into oxygen and aluminium orbitals and of the degree of covalency of this centre.

2. Experimental details

The $MgAl_2O_4$ samples used are from a natural origin and have a light violet colour. X-ray fluorescence and chemical analysis, respectively, provided the stoichiometry of these samples (molar ratio of $MgO:Al_2O_3$, 1:1.08), and main impurity contents (Fe, about 1000 ppm; Cr, Mn, about 100 ppm; V, about 3000 ppm; Zn, about 400 ppm).

The ENDOR measurements have been carried out at 4.2 K with a modified Varian E-1700 ENDOR spectrometer working in the X band. This apparatus employs a 20 W broad-band amplifier (ENI 420L) loaded by a three-turn coil (0.15 μH) placed inside the H_{102} microwave cavity. The loaded Q of this cavity is about 6000. Only a modulation of the RF field (range, 0.1–160 MHz) saturating the NMR transitions was employed without any additional modulation of the static magnetic field. The ENDOR spectra were measured with both amplitude and frequency modulation (Δf mode) of the saturating RF field [21]. In the Δf mode (differential pulse method) the RF signal from the frequency synthesizer is frequency modulated at 1 kHz and fed to the RF gate. The gate chops the frequency-modulated signal, but at 2 kHz. The difference between the frequency of the pulses is constant (Δf) as the average RF is swept. ENDOR signals such as the derivative of an absorption line are observed.

3. Results

3.1. EPR results

Although the electron paramagnetic resonance (EPR) spectra of Cr^{3+} in $MgAl_2O_4$ have been extensively investigated by several workers [22–27], further measurements were carried out at 300 and 4.2 K in order to identify the lines originating from

the Cr^{3+} ions and to determine the exact orientation of the natural samples in the magnetic field.

In the previous EPR studies the chromium ion was always found to occupy the B sites (figure 1). Moreover, several kinds of Cr centres in $MgAl_2O_4$ spinel were observed, one axial [22–24] and two orthorhombic [25, 26] Cr centres, as well as nearest-neighbour Cr^{3+} pairs [27]. The axial centre always gives rise to the most intense EPR signals. Our samples showed an intense EPR spectrum (linewidths, about 3 mT) without hyperfine structure, which has been attributed to the axial Cr centre [22–24]. The EPR spin-Hamiltonian parameters ($g_{\parallel} = 1.985$; $-g_{\perp} = 1.983$; $D = 0.915\ cm^{-1}$) given by Berger [24] allow us to explain the angular variations in our EPR spectra at 300 and 4.2 K, as shown in figure 2. Each of the four existing Cr centres has the trigonal distortion axis along a [111] crystal direction. Moreover, because of the large fine-structure parameter D, only one electronic transition gives rise to intense EPR lines, which has been identified as the $|\frac{1}{2}\rangle \leftrightarrow |-\frac{1}{2}\rangle$ in the low-field limit, since $D > 0$ [24].

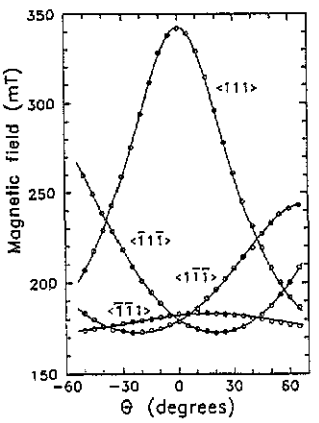

Figure 2. EPR angular variation at 4.2 K of the $|\frac{1}{2}\rangle \leftrightarrow |-\frac{1}{2}\rangle$ electronic transition of the Cr^{3+} ions in $MgAl_2O_4$: O, experimental magnetic field values; ——, theoretical values obtained with the EPR parameters given in the text. The magnetic field lies approxiamately in a plane which contains the $\langle 111 \rangle$ crystal direction, forming an angle θ with such direction. The EPR lines are labelled with the corresponding [111] principal axis of the chromium centre.

3.2. ENDOR results

ENDOR spectra have been obtained by saturation of the above-mentioned EPR transition for different orientations of the magnetic field along the four EPR angular variations shown in figure 2. They consist of two well separated sets of ENDOR lines in the regions from 5 to 10 MHz and from 20 to 50 MHz. Such sets are due to ^{27}Al and ^{53}Cr nuclei, respectively, and they will be described next.

3.2.1. Aluminium ENDOR spectra. The ENDOR spectra in figure 3 show clear quintets with peak-to-peak ENDOR linewidths of about 120 kHz and relative intensities close to 5:8:9:8:5. Each quintet corresponds to the five allowed transitions between the six hyperfine levels of one ^{27}Al nucleus or two magnetically equivalent ^{27}Al nuclei,

taking place in one electron spin state M_S. The splitting of the quintets results from quadrupole and second-order hyperfine interactions. The most intense ^{27}Al ENDOR line in figure 3(*a*) arises from a strong overlapping of lines and it splits for other magnetic field orientations. The angular dependences of the ENDOR spectrum in figure 4 show this effect well. Moreover, in this figure it is possible to observe that the ENDOR spectrum consists of three quintets. Therefore, as there are six aluminium nuclei surounding chromium, they must be equivalent in pairs.

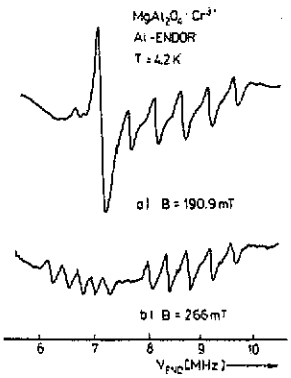

Figure 3. ENDOR spectra of ^{27}Al in natural $MgAl_2O_4$ single crystals with Cr^{3+} ions. The magnetic field is approximately forming an angle of (*a*) 58° with the $\langle\bar{1}1\bar{1}\rangle$ and 12° with the $\langle 111\rangle$ crystal directions and (*b*) 28° with the $\langle\bar{1}1\bar{1}\rangle$ and 88° with the $\langle 111\rangle$ crystal directions.

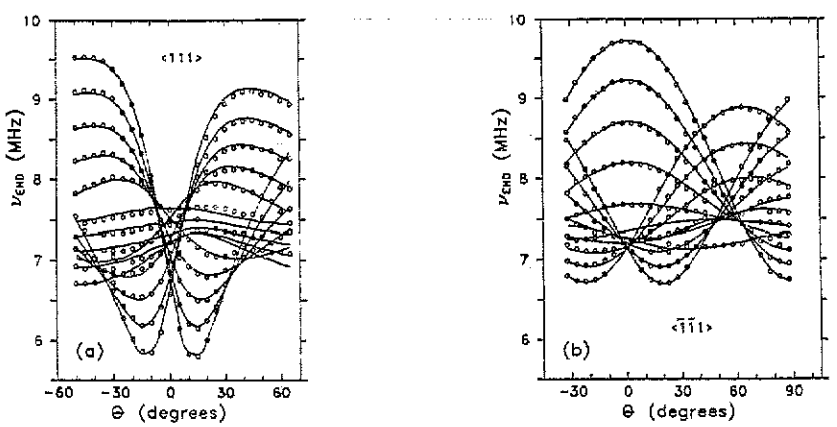

Figure 4. Angular variations in the ^{27}Al ENDOR spectrum obtained by saturation of the two EPR lines shown in figure 2: O, experimental ENDOR frequency values; ——, theoretical angular variations obtained by solving the spin Hamiltonian of (1) with the parameters given in table 1. θ is the angle between the magnetic field and the $\langle 111\rangle$ crystal direction.

On the other hand, it was not possible to observe the three other quintets which should arise from the other electron spin state. However, these ^{27}Al ENDOR lines are expected to occur in the region from 0 to 4 MHz, where the transition probabilities of the ENDOR signal are very low owing to the small enhancement factor.

The ENDOR frequencies with the selection rules $\Delta M_S = 0$, $\Delta M_I = \pm 1$, can be described by the following spin Hamiltonian for the six aluminium nuclei which surround chromium:

$$\hat{\mathcal{H}} = g_{\parallel}\beta B_Z \hat{S}_Z + g_{\perp}\beta(B_X \hat{S}_X + B_Y \hat{S}_Y) + D[\hat{S}_Z^2 - \tfrac{1}{3}S(S+1)] + \sum_{i=1}^{6}(\hat{S}\cdot \mathbf{A}_i \cdot \hat{I}_i + \hat{I}_i \cdot \mathbf{Q}_i' \cdot \hat{I}_i - g_n\beta_n B \cdot \hat{I}_i) \quad (1)$$

with $S = \frac{3}{2}$ the electron spin of Cr^{3+} and $I = \frac{5}{2}$ the nuclear spin of ^{27}Al. The first three terms of (1) correspond to the EPR Hamiltonian, which is expressed in the fine-structure axes system (X, Y, Z), with Z along the $\langle 111 \rangle$ crystal direction. The fourth and fifth terms describe the hyperfine and the quadrupole interactions, respectively. The corresponding two tensors have been assumed symmetric. The last term in (1) takes account of the nuclear Zeeman effect, where an isotropic factor g_n is used ($g_n = 1.4554$ for ^{27}Al).

To calculate the frequency values of the ENDOR lines the full 24×24 matrix which represents the spin Hamiltonian of (1) for one ^{27}Al nucleus has been exactly diagonalized by computer. This procedure is necessary because the first three terms in (1) influence considerably the ENDOR spectra due to the large value of the parameter D. Furthermore, a least-squares fitting method has been used to obtain the best estimates of the hyperfine and quadrupole tensors. In this procedure, four ENDOR angular variations of one ^{27}Al nucleus have been simultaneously fitted (figure 4 shows two of these angular variations). Table 1 gives the best set of parameters found for the electron spin state $M_S = -\frac{1}{2}$. The errors have been obtained by considering a 0.05 MHz uncertainty in the line position. The sign of the hyperfine interaction is obtained according to the sign of the parameter D. Moreover, the sign of the quadrupole interaction was determined by observing the intensity changes in the ENDOR lines of one quintet as the EPR signal was saturated at different points [28].

On the other hand, it should be pointed out that another different set of parameters, for the electron spin state $M_S = +\frac{1}{2}$ and $A_{iso} = -6.70$ MHz, also allows us to explain satisfactorily the experimental values observed. However, this set has been discarded since the theoretical frequencies corresponding to the non-observed electron spin state appear in the region from 0 to 7 MHz, but they have not been detected in the spectra. Moreover, the set of parameters shown in table 1 predicts the non-observed frequencies in the region from 0 to 4 MHz, which is unavailable to our spectrometer. Other reasons for choosing this set concern the resulting anisotropic hyperfine tensor, as well as the sign of the isotropic contstant A_{iso} predicted from covalency considerations, as discussed in section 4.2.

3.2.2. ^{53}Cr ENDOR spectra. In figure 5, a triplet is observed for each electron spin state corresponding to the three allowed transitions between the four hyperfine levels of ^{53}Cr. The ENDOR linewidth is about 200 kHz. Figure 6(*a*) shows the angular variation in the ^{53}Cr ENDOR spectrum obtained by saturation of the $\langle 111 \rangle$ EPR line shown in figure 2. A strong angular dependence of the ENDOR frequencies is observed near the $\langle 111 \rangle$ axis ($\theta = 0°$), where the spectra are complicated because of the overlapping of several lines, while 30° away from this direction it is smoother with clear spectra (see also figure 6(*b*)). This behaviour is due to the considerable influence of the fine-structure part on the ENDOR spectra.

Table 1. Principal components of the hyperfine and quadrupole tensors of the six ^{27}Al nuclei surrounding Cr^{3+} ions in natural $MgAl_2O_4$ spinel. The principal axes given correspond to nucleus 1 in figure 1. They are expressed by polar coordinates θ and ϕ and Miller indices, referred to the cubic crystal axes system (a, b, c). Inversion and rotations of 120° and 240° around the ⟨111⟩ axis provide the principal axes for the other nuclei.

Principal components		Principal axes		
Component	Value (MHz)	θ (deg)	ϕ (deg)	Miller indices
A_{iso}	5.63 ± 0.02			
B_{xx}	-0.94 ± 0.02	69 ± 5	114 ± 6	$\simeq \langle\bar{1}21\rangle$
B_{yy}	-1.02 ± 0.02	53 ± 4	220 ± 8	$\simeq \langle\bar{1}\bar{1}1\rangle$
B_{zz}	1.96 ± 0.03	44 ± 1	1 ± 1	$\simeq \langle 101\rangle$
Q'_{xx}	0.118 ± 0.007	64 ± 6	68 ± 6	$\simeq \langle 121\rangle$
Q'_{yy}	0.054 ± 0.007	48 ± 4	184 ± 7	$\simeq \langle\bar{1}01\rangle$
Q'_{zz}	-0.172 ± 0.009	53 ± 2	317 ± 2	$\simeq \langle 1\bar{1}1\rangle$

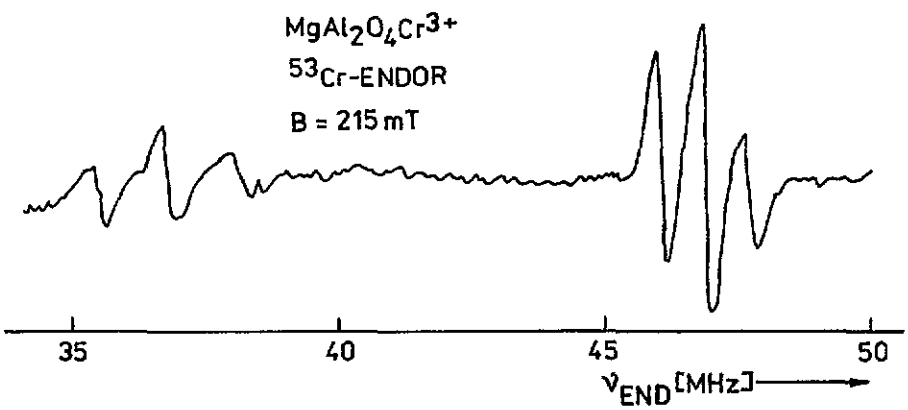

Figure 5. ENDOR spectrum of $^{53}Cr^{3+}$ in natural $MgAl_2O_4$ spinel recorded when the magnetic field is forming an angle of about 40° with the ⟨111⟩ crystal direction.

The allowed ENDOR frequencies can be described by the following axially symmetric spin Hamiltonian in the ground state of $^{53}Cr^{3+}$ ions ($S = \frac{3}{2}$; $I = \frac{3}{2}$):

$$\hat{\mathcal{H}} = g_{\parallel}\beta B_Z \hat{S}_Z + g_{\perp}\beta(B_X \hat{S}_X + B_Y \hat{S}_Y) + D[\hat{S}_Z^2 - \tfrac{1}{3}S(S+1)] + A\hat{S}_Z \hat{I}_Z + B(\hat{S}_X \hat{I}_X + \hat{S}_Y \hat{I}_Y) + Q'[\hat{I}_Z^2 - \tfrac{1}{3}I(I+1)] - g_{\parallel}^{n}\beta_n B_Z \hat{I}_Z - g_{\perp}^{n}\beta_n(B_X \hat{I}_X + B_Y \hat{I}_Y). \quad (2)$$

This spin Hamiltonian has been expressed in the fine-structure axes system, with Z along a [111] crystal direction. The first three terms are the same as in (1). The fourth and fifth terms describe the hyperfine interaction, the sixth term describes the quadrupole interaction, and the seventh and eighth terms describe the nuclear Zeeman effect.

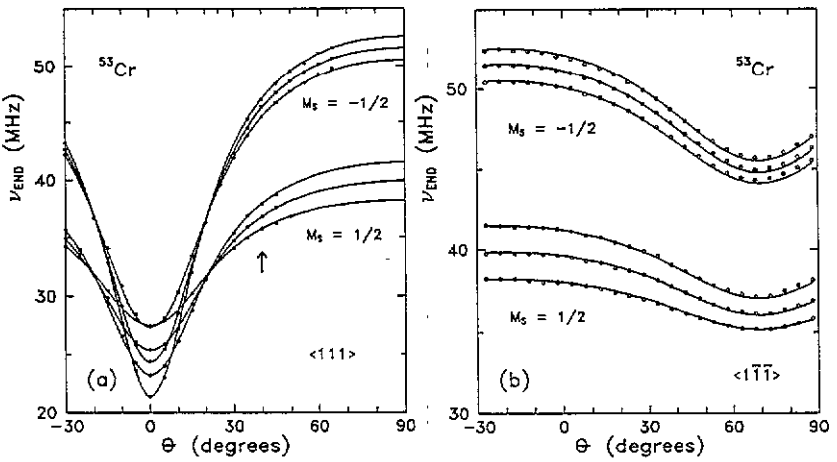

Figure 6. Angular variations in the ^{53}Cr ENDOR spectrum. The arrow in (*a*) indicates the spectrum shown in figure 5. O, experimental ENDOR frequency values; ——, theoretical angular variations obtained by solving (2) with the parameters given in table 2. M_S stands for the electronic spin state quantum number in the low-field limit.

Because of the large-D effects the 16 × 16 matrix which represents the complete Hamiltonian of (2) has been exactly diagonalized by computer, and a similar method to that in the case of ^{27}Al has been used to determine the hyperfine and quadrupole tensors (table 2). The signs of these tensors have been obtained using the procedure described in the previous section.

Table 2. Hyperfine and quadrupole parameters and nuclear g-values for $^{53}Cr^{3+}$ in natural $MgAl_2O_4$ spinel.

A MHz	B MHz	Q' MHz	$g_{\parallel}^{n}$	$g_{\perp}^{n}$
49.34 ± 0.04	46.49 ± 0.01	0.878 ± 0.006	−0.315 ± 0.008	−0.306 ± 0.008

4. Discussion and conclusions

Good agreement between experimental and theoretical ENDOR frequency values has been obtained, as observed in figures 4 and 6, which indicates that the preceding assumptions on the tensors and local symmetry of chromium for the spin Hamiltonians (1) and (2) are correct, as well as the nuclear factor g_n used for ^{27}Al. The nuclear factor g_n for ^{53}Cr has been found to be isotropic within experimental error, and its value is very close to the tabulated value (−0.3147).

4.1. ^{53}Cr hyperfine interaction

The magnitude of the isotropic hyperfine constant $A_{iso} = (A+2B)/3 = 47.44$ MHz is close to other values found in the literature for ^{53}Cr surrounded by six oxygen ions [29–31], and its positive sign is also in accordance with these studies, which

ensures a positive sign for the fine-structure parameter D. The constant A_{iso} is related to the fraction of unpaired spin density present on the Cr^{3+} ion, which can be obtained by comparison with the free-ion value. Simánek and Müller [32] estimated a value of -25 T for the hyperfine field per electron spin in the case of the isoelectronic free V^{2+} ion. Therefore, a value of 60 MHz is obtained for the isotropic constant of the free $^{53}Cr^{3+}$ ion. So, a fraction of unpaired spin density of 0.79 is estimated on the Cr^{3+} ion in $MgAl_2O_4$.

On the other hand, as shown by McGarvey [33], the hyperfine parameters A and B can be described from first-order perturbation theory by the following expressions:

$$\begin{aligned} A &= P[\tfrac{4}{21}(1 - 2a^2 + b^2) - K] \\ B &= P[-\tfrac{2}{21}(1 - 2a^2 + b^2) - K] \end{aligned} \tag{3}$$

where $P = -40 \times 10^{-4}$ cm^{-1} for $^{53}Cr^{3+}$, K is related to A_{iso} through $A_{iso} = -PK$, and $1 - 2a^2 + b^2$ arises from the electron–nuclear dipole–dipole interaction, where $a^2 + b^2 = 1$. When the symmetry is octahedral, $a^2 = \frac{2}{3}$, giving $A = B$. In our case the values of A and B (table 2) give $a^2 = 0.694$ which is larger than $\frac{2}{3}$ as $A > B$. McGarvey [33] has shown that the parameter D is negative when $A < B$, and the coordinated octahedron is trigonally compressed, with $a^2 < \frac{2}{3}$. Therefore, in this framework it follows that the relation $A > B$ ($a^2 > \frac{2}{3}$) corresponds to a positive D-value and a trigonal extension of the octahedron, according to Manoogian and Leclerc [31]. This result is consistent with the sign of D and shows that the Cr^{3+} ion is subjected to the original trigonal expansion at the B sites.

4.2. ^{27}Al hyperfine interaction

The anisotropic part of the ^{27}Al hyperfine interaction is almost axial (see table 1), and the principal axis which corresponds to the largest component B_{zz} points from chromium towards aluminium 1 in figure 1. In a point-dipole model, B_{zz} is given by

$$B_{zz} = 2gg_n\beta\beta_n/R^3 \tag{4}$$

which, with $R = 2.857$ Å (see caption for figure 1), provides a value $B_{zz} = 1.76$ MHz. Moreover, if corrections due to covalent transfer of the magnetic ion spin onto the oxygen ligands are taken into account [34], then the former value is estimated to be larger by about 10%, i.e. $B_{zz} = 1.94$ MHz. This value accounts for most of the measured hyperfine anisotropy shown in table 1. The small orthorhombicity observed in this tensor would originate from some unpaired spin density in aluminium 2p orbitals.

The value of the isotropic constant A_{iso} shown in table 1 is due to some unpaired spin density on Al^{3+} s orbitals. It can be explained from an independent bonding model [35], taking into account the nearest-neighbour structures formed by Cr^{3+} and Al^{3+} at the corners of a square, and two oxygen ions such as O_1^{2-} and O_2^{2-}, as shown in figure 1 and in more detail in figure 7.

The unpaired electrons on the sixfold-coordinated Cr^{3+} ion have the configuration $3d^3(t_{2g}^3)$, without unpaired electrons on e_g orbitals (not shown in figure 7). The first step for transferring unpaired spin from Cr^{3+} and Al^{3+} consists of electron transfer from O^{2-} to Cr^{3+} and π overlap, which leaves a positive unpaired spin density f_π in

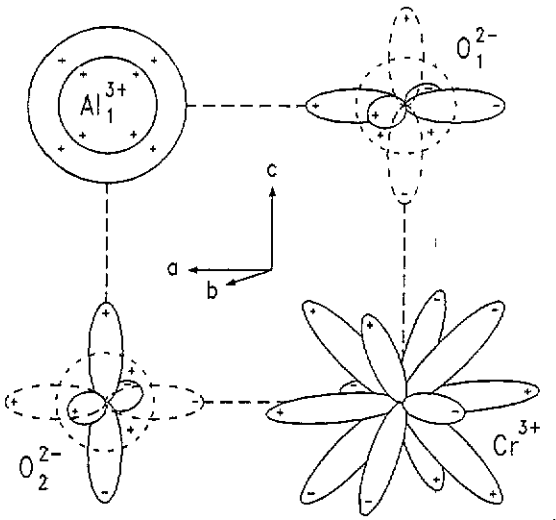

Figure 7. Relevant orbitals considered in the analysis of the ^{27}Al isotropic hyperfine interaction. The depicted orbitals are the t_{2g} orbitals d_{ab}, d_{ac} and D_{bc} on Cr^{3+}, the 2s, $2p_a$, $2p_b$ and $2p_c$ on the O^{2-} ions, and the 2s and 3s orbitals on Al^{3+}. The orbitals shown as broken curves on oxygen ions do not provide any overlap path (see text).

$2p_\pi$ orbitals on O^{2-} [35]†. Second, one lobe of $2p_\pi$ orbitals per each O^{2-} overlaps with the 2s orbitals on Al^{3+}, causing an unpaired spin density on them which is given by $f_\pi S^2_{\sigma 2s'}$ where $S_{\sigma 2s}$ is the σ overlap integral between $2p_\pi$ orbitals on O^{2-} and 2s orbitals on Al^{3+}. Therefore, this contribution to the isotropic hyperfine constant from one oxygen ion is given by

$$A_{iso}(2s)/2 = f_\pi S^2_{\sigma 2s} A_{2s}/2S \tag{5}$$

where $A_{2s} = 51\,400$ MHz is the Fermi contact term for a single unpaired electron in one Al^{3+} 2s orbital [36]. f_π can be estimated from the fraction of unpaired spin density on the Cr^{3+} ion determined in section 4.1. On account of the six first-neighbour oxygen ions of Cr^{3+} it is considered that each $2p_\pi$ lobe orbital on O^{2-} has a fraction $(1 - 0.79)/12$ of unpaired spin density, i.e. $f_\pi = 0.0175$. Therefore, using (5) with $S_{\sigma 2s} = 0.094$ as calculated by Taylor *et al* [28] for similar distances between O^{2-} and Al^{3+}, a value of $A_{iso}(2s) = 5.30$ MHz is calculated. This value agrees very well with the measured value (table 1).

However, Taylor *et al* [28] have shown that there is a non-negligible 2s–3s cross term contribution to A_{iso}. On our case the expression given in [28] for such a contribution is

$$A_{iso}(2s - 3s)/2 = -(2a_{\pi d} a_{\sigma 3s} S_{\sigma 2s} S_{\pi d} + a_{\sigma 3s} S_{\sigma 2s} S^2_{\pi d})/(A_{2s,3s}/2S) \tag{6}$$

where $A_{2s,3s} = -14300$ MHz, the overlap integral $S_{\pi d} = 0.066$ and the transfer parameter $a_{\sigma 3s} = 0.155$ have been taken from [28]. The transfer parameter

† The 2s and $2p_\sigma$ orbitals on O^{2-} (shown by broken curves in figure 7) will no longer be considered because they have zero overlap with the t_{2g} orbitals on Cr^{3+} and the negative spin density induced in such orbitals due to exchange polarization with empty orbitals on Cr^{3+} is not very significant in our case. For instance, the negative unpaired $2p_\sigma$ density is typically about $f_\pi/10$ [36].

$a_{\pi d} = 0.066$ is obtained from $f_\pi = (a_{\pi d} + S_{\pi d})^2$. Using (6) with these values and $S_{\sigma 2s}$ given above, the value $A_{iso}(2s-3s) = 1.82$ MHz is obtained, i.e. the total value is $A_{iso} = 7.12$ MHz. However, it should be pointed out that the overlap integrals used involve some uncertainty, and that the Al^{3+} 1s orbital has been omitted but gives rise to a negative 1s–2s cross term [36] which reduces the resulting s density.

The above covalency considerations also explain the positive sign of the isotropic constant and, therefore, confirm that the set of parameters shown in table 1 is correct and the observed ENDOR transitions take place in the electron spin state $M_S = -\frac{1}{2}$.

4.3. Quadrupole interactions

The constant Q' for the axial quadrupole interaction of ^{53}Cr can be written in terms of the quadrupole moment eQ of ^{53}Cr as

$$Q' = [3V_{ZZ}eQ/4I(2I-1)]/(1-\eta) \tag{7}$$

where V_{ZZ} is the electric field gradient external to the Cr^{3+} ion, and $1-\eta = 12.0$ is the Sternheimer antishielding factor for Cr^{3+} [31]. Using the value $eQ = -0.0285$b, $I = \frac{3}{2}$ and the experimental value for Q' in table 2, a value $V_{ZZ} = -3.43 \times 10^{-4}$ cm^{-1}/b is obtained.

On the other hand, the ^{27}Al quadrupole tensor shows a considerable orthorhombic character (table 1), and equation (7) cannot be used directly. The orthorhombicity can be explained by considering that this interaction is built up of two parts. The first part Q'^{ax} would be due to the original field gradient at the B sites, which for aluminium 1 in figure 1 is directed along the $\langle 1\bar{1}1\rangle$ axis. The second part Q'^{cov} is expected to be a covalent contribution to the field gradient, which originates from differences between the occupancies q_σ and q_π of aluminium 2p orbitals due to the chromium effect, as proposed by Taylor *et al* [28]. The value of Q'^{ax} was measured in natural $MgAl_2O_4$ by Brun and Hafner [37], who obtained $Q'^{ax} = \pm 0.276$ MHz. Therefore, taking the negative sign for Q'^{ax}, the covalent contribution would have the components $Q'^{cov}_{zz} = 0.104$ MHz, $Q'^{cov}_{yy} = -0.084$ MHz and $Q'^{cov}_{xx} = -0.020$ MHz, along the directions given in table 1. In this case the absolute value of Q'^{cov} is similar to that measured for $LaAlO_3$:Cr^{3+} by Taylor *et al* [28]. Now it is possible to use equation (7) with the negative value of Q'^{ax}, the quadrupole moment of ^{27}Al ($eQ = 0.149$b), the antishielding factor for ^{27}Al $1-\eta = 3.36$ [31] and $I = \frac{5}{2}$, to obtain the electric gradient external to the Al^{3+} ion. The result is $V_{zz} = -2.45 \times 10^{-4}$ cm^{-1}/b. The sign of this value agrees with the negative sign of the field gradient at the Cr site obtained above, and the magnitude is 70% of this. This result indicates that, although chromium is subjected to the original expansion at the B sites, as discussed in section 4.1, some distortion effects are expected to occur because the ionic radius of Cr^{3+} (0.63 Å) is slightly greater than that of Al^{3+} (0.51 Å).

4.4. Point symmetry of Cr^{3+} ions

Since only three quintets have been observed in the ^{27}Al ENDOR spectra, the Cr^{3+} ion should be located at an inversion centre. However, if the experimental ENDOR linewidth is taken into account, a possible small displacement of chromium along the $\langle 111\rangle$ direction must be considered, as suggested by several workers [18–20]. In this case, the aluminium ions are not exactly equivalent in pairs, and they would give rise to a broadening of the ENDOR lines. As the ENDOR linewidth is about 120 kHz, a

maximum difference in the line position of about 60 kHz is estimated for the two nearly equivalent aluminium nuclei. To explain such a possible difference a point-dipole model has been used, and a maximum displacement for chromium of 0.03 Å has been obtained. In this case the difference between the two line positions ranges from 60 to 0 kHz along a theoretical angular variation. However, the experimental ENDOR linewidth has been found to be invariably constant for all magnetic field orientations. Therefore, it is concluded that the linewidth is not related to slightly inequivalent nuclei, and that the point symmetry of chromium in natural $MgAl_2O_4$ spinel is $\bar{3}m$ (D_{3d}).

Moreover, as shown by Schmocker and Waldner [2], the inversion parameter for natural $MgAl_2O_4$ crystals is usually very small (about 0.04), and most of the Cr^{3+} ions would be surrounded by six Al^{3+} ions. Therefore, our result suggests that the point group $\bar{3}m$ and the space group $Fd3m$ are related to low values of the inversion parameter. This is supported by the proposal of Schmocker and Waldner [2], who have considered that the displacement of a cation in $MgAl_2O_4$ is the result of the actual cation distribution present in the surroundings of this cation.

Acknowledgments

The authors are indebted to Dr A Ibarra (EURATOM–CIEMAT Association, Madrid) for supplying the samples.

References

[1] Gray T J 1971 *High Temperature Oxides* (New York: Academic) part IV
[2] Schmocker U and Waldner F 1976 *J. Phys. C: Solid State Phys.* **9** L235–7
[3] Heuer A H and Mitchell T E 1975 *J. Phys. C: Solid State Phys.* **8** L541–3
[4] Grimes N W, Thompson P and Kay H F 1983 *Proc. R. Soc.* A **386** 33–8
[5] Grimes N W 1972 *Phil. Mag.* **26** 1217–26
[6] Hwang L, Heuer A H and Mitchell T E 1973 *Phil. Mag.* **28** 241–3
[7] Grimes N W 1973 *J. Phys. C: Solid State Phys.* **6** L78–9
[8] Jagodzinski H and Saalfeld H 1958 *Z. Kristallogr.* **110** 197–218
[9] Thompson P and Grimes N W 1977 *J. Appl. Crystallogr.* **10** 369–71
[10] Mishra R K and Thomas G 1977 *Acta Crystallogr.* A **33** 678
[11] Staszak P R, Poetzinger J E and Wirtz G P 1984 *J. Phys. C: Solid State Phys.* **17** 4751–7
[12] Chang Z P and Barsch G R 1973 *J. Geophys. Res.* **78** 2418–33
[13] DeCooman B C and Carter C B 1985 *Phil. Mag.* A **51** 175–7
[14] Smith P P K 1978 *Phil. Mag.* B **38** 99–102
[15] Samuelsen E J and Steinsvoll O 1975 *J. Phys. C: Solid State Phys.* **8** L427–9
[16] Tokonami M and Horiuchi H 1980 *Acta Crystallogr.* A **36** 122–6
[17] Steinsvoll O and Samuelsen E J 1981 *Phys. Scr.* **24** 57–8
[18] Lou F H and Ballentyne D W G 1968 *J. Phys. C: Solid State Phys.* **1** 608–13
[19] Grimes N W 1971 *J. Phys. C: Solid State Phys.* **4** L342–4
[20] Grimes N W and Collett A J 1971 *Phys. Status Solidi* b **43** 591–9
[21] Hyde J S 1965 *J. Chem. Phys.* **43** 1806–18
[22] Stahl-Brada R and Low W 1959 *Phys. Rev.* **116** 561–4
[23] Atsarkin V A 1963 *Soviet Phys.–JETP* **16** 593–6
[24] Berger S B 1965 *J. Appl. Phys.* **36** 1048–9
[25] Schmocker U, Boesch H R and Waldner F 1972 *Phys. Lett.* **40A** 237–8
[26] van den Boom H and Henning J C M 1973 *J. Phys. Chem. Solids* **34** 1211–16
[27] Henning J C M and van den Boom H 1973 *Phys. Rev.* B **8** 2255–62
[28] Taylor D R, Owen J and Wanklyn B M 1973 *J. Phys. C: Solid State Phys.* **6** 2592–610

[29] Terhune R W, Lambe J, Kikuchi C and Baker J 1961 *Phys. Rev.* **123** 1265–8
[30] Danilov A G and Manoogian A 1972 *Phys. Rev.* B **6** 4103–11
[31] Manoogian A and Leclerc A 1974 *Phys. Rev.* B **10** 1052–8
[32] Simánek E and Müller K A 1970 *J. Phys. Chem. Solids* **31** 1027–40
[33] McGarvey B R 1964 *J. Chem. Phys.* **40** 809–12
[34] Marshall W and Stuart R 1961 *Phys. Rev.* **123** 2048–58
[35] Owen J and Thornley J H M 1966 *Rep. Prog. Phys.* **29** 675–728
[36] Geschwind S 1972 *Electron Paramagnetic Resonance* (New York: Plenum) ch 8
[37] Brun E and Hafner S 1962 *Z. Kristallogr.* **117** 37–78